

# Shear instability in a stratified fluid when shear and stratification are not aligned

Julien Candelier<sup>1,2,†</sup>, Stéphane Le Dizès<sup>2</sup> and Christophe Millet<sup>1</sup>

<sup>1</sup> CEA, DAM, DIF, F-91297 Arpajon, France

<sup>2</sup> IRPHE, CNRS and Aix–Marseille University, 49 rue F. Joliot-Curie, F-13013 Marseille, France

(Received 1 September 2010; revised 3 June 2011; accepted 8 July 2011;  
first published online 13 September 2011)

The effect of an inclination angle of the shear with respect to the stratification on the linear properties of the shear instability is examined in the work. For this purpose, we consider a two-dimensional plane Bickley jet of width  $L$  and maximum velocity  $U_0$  in a stably stratified fluid of constant Brunt–Väisälä frequency  $N$  in an inviscid and Boussinesq framework. The plane of the jet is assumed to be inclined with an angle  $\theta$  with respect to the vertical direction of stratification. The stability analysis is performed using both numerical and theoretical methods for all the values of  $\theta$  and Froude number  $F = U_0/(LN)$ . We first obtain that the most unstable mode is always a two-dimensional Kelvin–Helmholtz (KH) sinuous mode. The condition of stability based on the Richardson number  $Ri > 1/4$ , which reads here  $F < 3\sqrt{3}/2$ , is recovered for  $\theta = 0$ . But when  $\theta \neq 0$ , that is, when the directions of shear and stratification are not perfectly aligned, the Bickley jet is found to be unstable for all Froude numbers. We show that two modes are involved in the stability properties. We demonstrate that when  $F$  is decreased below  $3\sqrt{3}/2$ , there is a ‘jump’ from one two-dimensional sinuous mode to another. For small Froude numbers, we show that the shear instability of the inclined jet is similar to that of a horizontal jet but with a ‘horizontal’ length scale  $L_h = L/\sin\theta$ . In this regime, the characteristics (oscillation frequency, growth rate, wavenumber) of the most unstable mode are found to be proportional to  $\sin\theta$ . For large Froude numbers, the shear instability of the inclined jet is similar to that of a vertical jet with the same scales but with a different Froude number,  $F_v = F/\cos\theta$ . It is argued that these results could be valid for any type of shear flow.

**Key words:** jets, parametric instability, stratified flows

## 1. Introduction

Shear instability is one of the most famous instabilities in fluid dynamics. Despite the enormous number of papers concerning this instability, fundamental results such as the effect of uniform stratification on the linear growth of the instability are still absent. Stable stratification is known to be stabilizing when the direction of stratification is aligned along with the shear. It is also known to have no effect when it is perpendicular. But little is known when one is inclined with respect to the other. In this work, we want to analyse how the stability properties vary when

<sup>†</sup> Email address for correspondence: [candelierj@gmail.com](mailto:candelierj@gmail.com)

we pass from the vertical shear to the horizontal shear situation. We consider the idealized configuration of a two-dimensional plane Bickley jet in a stably stratified fluid of constant Brunt–Väisälä frequency  $N$  when the plane of the shear makes an angle  $\theta$  with respect to the direction of the stratification. We provide the stability characteristics properties of such a jet for any angle and stratification.

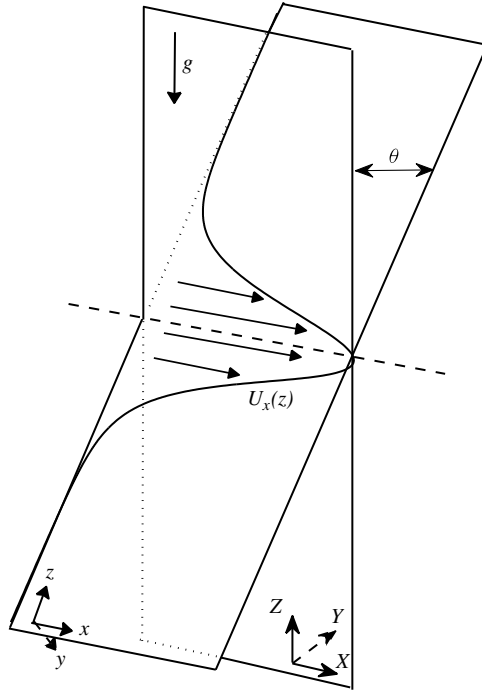
Most stability analyses have been performed for configurations where shear and stratification are aligned in the same vertical direction. Miles (1961) and Howard (1961) demonstrated that in that case the stability properties of the flow are mainly governed by the Richardson number  $Ri = (N/U_z)^2$ , where  $U_z$  is the vertical derivative of the velocity field, which has to be smaller than  $1/4$  for instability. Booker & Bretherton (1967) have shown that when  $Ri > 1/4$ , internal gravity waves are attenuated as they pass across a shear layer. In contrast, for  $Ri < 1/4$ , a mechanism of over-reflection is active, which can explain the instability (e.g. Acheson 1976; Lindzen & Barker 1985).

The shear instability in a homogeneous fluid is a two-dimensional instability (e.g. Drazin & Reid 1981). Thanks to this property, the most unstable mode found in a homogeneous fluid is not affected by a stratification oriented perpendicular to the plane of the shear. Consequently, this mode is expected to be present in a horizontal shear flow for any stratification strength. This property was also observed in more complex shear flows. Blumen (1971, 1975) observed that when the shear flow is non-planar but separable, both instabilities associated with horizontal shear and vertical shear could be present simultaneously.

The three-dimensional stability properties of a horizontal shear flow have been analysed by Deloncle, Chomaz & Billant (2007). They have demonstrated that the most unstable mode remains two-dimensional for both hyperbolic tangent shear layers and Bickley jets. Nevertheless, they have also shown that strong stratification has an effect on the three-dimensional character of the instability by making the width of the associated wavenumber band proportional to  $N$ . In a companion paper (Candelier 2010), we show that a horizontal Bickley jet also exhibits other less unstable three-dimensional modes. These modes are similar to those found in supersonic jets (Mack 1990; Luo & Sandham 1997; Parras & Le Dizès 2010). The mechanism of instability of these modes is different from the shear instability and associated with the phenomenon of over-reflection (Basovich & Tsimring 1984; Le Dizès & Billant 2009).

The effect of the inclination of the shear with respect to the stratification has also been analysed in a turbulence context. By considering an unbounded constant shear configuration, Jacobitz & Sarkar (1998, 1999) have shown that horizontal shear tends to make turbulence more energetic than vertical shear. Basak & Sarkar (2006) have analysed the nonlinear dynamics of a horizontal shear layer and shown that it strongly differs from the homogeneous case.

The paper is organized as follows. In § 2, the base flow and the perturbation equations are provided. The numerical method and the issues associated with the boundary conditions are also discussed. In § 3, the asymptotic regimes of small or large Froude numbers are considered. In § 4, the numerical stability results are presented. We analyse how the two-dimensional sinuous Kelvin–Helmholtz (KH) mode, which remains the most unstable mode, is modified as the inclination angle  $\theta$  is varied. We show that this mode is unstable for any Froude number when  $\theta \neq 0$ . The spatial structure of the mode is also provided in this section. In the last section, the main results are briefly summarized.


 FIGURE 1. Sketch of the base flow and definition of the angle  $\theta$ .

## 2. Base flow and perturbation equations

We consider a two-dimensional Bickley jet in a stably stratified, non-rotating, inviscid fluid under Boussinesq approximation. The flow has a velocity field given by

$$U(z)\mathbf{e}_x = U_0/\cosh^2(z/L)\mathbf{e}_x, \quad (2.1)$$

where  $\mathbf{e}_x$  is the unit vector in the  $x$ -direction. The fluid is characterized by a constant Brunt–Väisälä frequency  $N$  defined by  $N^2 = -g\bar{\rho}_Z/\rho_0$ , where  $g$  is gravity,  $Z$  is the upward vertical direction,  $\rho_0$  is a constant reference density and  $\bar{\rho}_Z$  is the derivative of the mean density with respect to  $Z$ . The flow is two-dimensional and its  $(x, z)$  shear plane is assumed to make an angle  $\theta$  with respect to the direction of stratification  $Z$ , as shown in figure 1.

All the variables are non-dimensionalized with the maximal velocity  $U_0$ , the jet width  $L$  and the reference density  $\rho_0$ . The base flow is then defined by two parameters: the Froude number  $F = U_0/(LN)$  and the angle  $\theta$ . It is also useful to introduce a vertical Froude number  $F_v = U_0/(LN \cos \theta)$ , and a Richardson number  $Ri$  based on the maximum shear gradient  $dU/dz$ . For the Bickley jet, one can easily obtain  $Ri = (3\sqrt{3})^2/(4F)^2$ , so that the stability condition  $Ri > 1/4$  for a vertical jet is equivalent to  $F < 3\sqrt{3}/2$ .

Local stability properties are obtained by considering perturbations of velocity  $\mathbf{u}' = (u', v', w')$ , pressure  $p'$  and density  $\rho'$  as a plane wave

$$(\mathbf{u}', p', \rho') = (\mathbf{u}, p, \rho) \exp(ik_x x + ik_y y - i\omega t), \quad (2.2)$$

where  $k_x$  and  $k_y$  are real wavenumbers in the streamwise and spanwise directions and  $\omega = \omega_r + i\omega_i$  is the complex frequency. The real part  $\omega_r$  is the oscillation frequency and the imaginary part  $\omega_i$  defines the growth rate. The perturbation equations are obtained by linearizing the Euler equations around the base flow (2.1) under the Boussinesq approximation. These equations can readily be written as

$$-i\phi u + U_z w = -ik_x p, \quad (2.3a)$$

$$-i\phi v + \sin\theta b = -ik_y p, \quad (2.3b)$$

$$-i\phi w - \cos\theta b = -\frac{dp}{dz}, \quad (2.3c)$$

$$-i\phi b - \frac{\sin\theta}{F^2} v + \frac{\cos\theta}{F^2} w = 0, \quad (2.3d)$$

$$ik_x u + ik_y v + \frac{dw}{dz} = 0, \quad (2.3e)$$

where  $\phi = \omega - k_x U$  is the inertial frequency of the perturbation,  $U_z$  is the derivative with respect to  $z$  of the base flow velocity  $U$ , and  $b = -g\rho/\rho_0$  is the buoyancy perturbation. By eliminating  $u$ ,  $v$ ,  $w$  and  $b$  from (2.3), a single equation for  $p$  can be found:

$$(\bar{\phi}^2 - \sin^2\theta) \frac{\partial^2 p}{\partial z^2} + \left[ -2\bar{\phi}_z \frac{(2\bar{\phi}^2 - 1)\sin^2\theta - \bar{\phi}^4}{\bar{\phi}(1 - \bar{\phi}^2)} - 2ik_y \sin\theta \cos\theta \right] \frac{\partial p}{\partial z} + \left[ k_y^2(\cos^2\theta - \bar{\phi}^2) + k_x^2(1 - \bar{\phi}^2) - 2ik_y \bar{\phi}_z \sin\theta \cos\theta \frac{2\bar{\phi}^2 - 1}{\bar{\phi}(1 - \bar{\phi}^2)} \right] p = 0, \quad (2.4)$$

where  $\bar{\phi} = \phi F$  and  $\bar{\phi}_z = -Fk_x U_z$ .

The boundary condition at infinity is that  $p$  is evanescent or a wave propagating outward. This condition can be analysed by considering the possible behaviours of the solutions near infinity. These behaviours can be obtained from (2.4) by expanding the coefficient near infinity and searching for formal solutions in the form  $\exp(i\beta z)$ . This gives an equation for  $\beta$ ,

$$-(\bar{\omega}^2 - \sin^2\theta)\beta^2 + 2k_y \sin\theta \cos\theta \beta + k_y^2(\cos^2\theta - \bar{\omega}^2) + k_x^2(1 - \bar{\omega}^2) = 0, \quad (2.5)$$

which can be solved as follows:

$$\beta^\pm = \frac{-k_y \sin\theta \cos\theta \pm \sqrt{(1 - \bar{\omega}^2)[\bar{\omega}^2(k_x^2 + k_y^2) - k_x^2 \sin^2\theta]}}{\sin^2\theta - \bar{\omega}^2}, \quad (2.6)$$

where  $\bar{\omega} = \omega F$ .

These two functions  $\beta^\pm$  depend on  $\bar{\omega}^2$  only. They possess two branch points at  $\bar{\omega}_0^2$  and  $\bar{\omega}_2^2$  and a pole at  $\bar{\omega}_1^2$ , where

$$\bar{\omega}_0^2 = \frac{k_x^2 \sin^2\theta}{k_x^2 + k_y^2}, \quad \bar{\omega}_1^2 = \sin^2\theta \quad \text{and} \quad \bar{\omega}_2^2 = 1. \quad (2.7)$$

If we choose the branch cut between  $\bar{\omega}_0^2$  and  $\bar{\omega}_2^2$ , one can define  $\beta^+$  and  $\beta^-$  such that  $0 < \arg(\beta^+) < \pi$  and  $-\pi < \arg(\beta^-) < 0$  in the upper half-plane  $\bar{\omega}_i > 0$ . The eigenvalue problem is then well-posed (that is, discrete) in the upper half-plane: the wavenumbers  $\beta^+$  and  $\beta^-$  correspond to the wavenumbers of the solutions which satisfy the boundary

condition at  $+\infty$  and  $-\infty$  respectively. On the branch cut, that is, for

$$\bar{\omega}_0^2 \leq \bar{\omega}^2 \leq \bar{\omega}_2^2, \quad (2.8)$$

the wavenumbers  $\beta^+$  and  $\beta^-$  obtained by analytic continuation are real and represent outgoing waves in  $+\infty$  and  $-\infty$  respectively. For these frequencies, the eigenmode has an oscillating behaviour at  $|z| \rightarrow \infty$ , which means that it is radiating.

For horizontal ( $\theta = \pi/2$ ) and vertical ( $\theta = 0$ ) shear, the perturbations satisfy symmetry properties and can be split into sinuous and varicose modes. Sinuous modes possess odd  $u$ ,  $v$  and  $p$  and even  $w$ , whereas varicose modes have even  $u$ ,  $v$  and  $p$ , and odd  $w$ . The parity of  $\rho$ , however, depends on the direction of the shear: it has the parity of  $w$  for vertical shear ( $\theta = 0$ ) but the opposite parity for horizontal shear ( $\theta = \pi/2$ ). For three-dimensional modes ( $k_x \neq 0$  and  $k_y \neq 0$ ), as soon as  $\theta$  differs from 0 and  $\pi/2$ , there is no longer symmetry, and the eigenmodes are neither sinuous nor varicose. However, for two-dimensional modes ( $k_y = 0$ ) symmetry is present for all  $\theta$ .

For the numerical resolution, the system of (2.3) is written in matrix form,

$$\mathbf{A} = \omega \mathbf{B}, \quad (2.9)$$

so that the three-dimensional stability of the Bickley jet is determined by computing all the eigenvalues of the matrix operator. The two operators  $\mathbf{A}$  and  $\mathbf{B}$  are discretized using Chebyshev polynomials interpolating at the Gauss–Lobatto collocation points. The algebraic transformation  $z \mapsto \tilde{z}/(1 - \tilde{z}^2)$  is used to map the unbounded domain to the interval  $-1 < \tilde{z} < 1$ . A complex integration path  $z = \hat{z}e^{i\epsilon}$  is also implemented to be able to capture radiating solutions and to avoid the critical points such that  $\omega - k_x U = 0$ ,  $\omega - k_x U = \pm 1/F$  and  $\omega - k_x U = \pm \sin \theta / F$ . Furthermore, the perturbations' parity can be exploited by considering only half of the Chebyshev polynomials and then twice as few collocation points. More details on the integration technique and the complex path trick can be found in Riedinger, Le Dizès & Meunier (2010).

### 3. Asymptotic regimes

For a strongly stratified medium, the stability characteristics of the jet satisfy a few properties that can be deduced from (2.4). If we assume that both  $F$  and  $F/\sin \theta$  are small, (2.4) can be reduced to leading order in  $F$  to a simpler equation for  $q(r) = \exp(ik_y z / \tan \theta) p(r)$ :

$$\frac{\partial^2 q}{\partial z^2} + \frac{2U_z}{c_x - U} \frac{\partial q}{\partial z} + \frac{k_x^2}{\sin^2 \theta} \left[ \frac{k_y^2 F^2}{\sin^2 \theta} (c_x - U)^2 - 1 \right] q = 0, \quad (3.1)$$

where  $c_x = \omega/k_x$  is the streamwise phase velocity. This equation guarantees that for small  $F/\sin \theta$  the eigenvalue  $c_x$  depends on the four parameters  $F$ ,  $\theta$ ,  $k_x$  and  $k_y$  via only two quantities  $k_x/\sin \theta$  and  $k_y F/\sin \theta$ . This has important consequences for the variations of the stability property of the jet with respect to the angle  $\theta$  and  $F$  for small Froude numbers. For example, for two-dimensional modes ( $k_y = 0$ ), this implies that the dispersion relation satisfies

$$\omega(k_x, F, \theta) \sim \omega(k_x/\sin \theta, 0, \pi/2) \sin \theta, \quad (3.2)$$

when  $F/\sin \theta$  is small. This also implies that the maximum growth rate is given by a relation of the form

$$\omega_i^{\max}(\theta, F) \sim \omega_i^{\max}(\pi/2, 0) \sin \theta, \quad (3.3)$$

if  $F/\sin\theta$  is small. We shall see below that this relation provides a good approximation of the growth rate of two-dimensional modes for  $F/\sin\theta < 1$ . Physically, relation (3.2) means that, for small  $F/\sin\theta$ , the stability properties of an inclined jet are the same as those of a horizontal jet but with a rescaled characteristic length scale  $L_h = L/\sin\theta$ .

For a weakly stratified medium, a similar analysis can be performed for two-dimensional modes. If we expand (2.4) for two-dimensional modes ( $k_y = 0$ ) in the limit of large  $F$ , we obtain up to  $O(1/F^4)$  terms:

$$\frac{\partial^2 p}{\partial z^2} - 2\frac{\phi_z}{\phi} \left(1 + \frac{\cos^2\theta}{F^2\phi^2}\right) \frac{\partial p}{\partial z} - k_x^2 \left(1 - \frac{\cos^2\theta}{F^2\phi^2}\right) p = 0. \quad (3.4)$$

In this equation, the base flow parameters  $\theta$  and  $F$  appear in the single combination  $F/\cos\theta$ . This implies that in the weakly stratified regime, two-dimensional modes are expected to possess a dispersion relation of the form

$$\omega(k_x, F, \theta) \sim \omega(k_x, F_v, 0), \quad (3.5)$$

where  $F_v = F/\cos\theta$  is a ‘vertical’ Froude number. This relation means that for large  $F$ , the two-dimensional stability properties of an inclined jet are the same as a vertical jet but with a different Froude number,  $F_v = F/\cos\theta$ .

It is worth mentioning that these two asymptotic regimes do not depend on the particular form of our base flow profile. They are expected to be valid for any plane shear flow. In particular, they should also apply to shear layers and wakes.

#### 4. Numerical results

The stability analysis is performed by searching the eigenfrequency with the largest growth rate for fixed perturbation wavenumbers  $k_x$  and  $k_y$  and fixed base flow parameters  $\theta$  and  $F$ . A typical plot of the maximum growth rate contours in the wavenumber plane is shown in figure 2. On this plot, we can see that the most unstable mode among all  $k_x$  and  $k_y$  is obtained for  $k_x \approx 0.9$  and  $k_y = 0$ . It corresponds to the classical two-dimensional sinuous Kelvin–Helmholtz (KH) mode (see the mode structure in figure 6d) which is known to be the most unstable in a homogeneous fluid. We recover here the result obtained by Deloncle *et al.* (2007).

The parameters  $F$  and  $\theta$  have been systematically varied. The first important result that we have obtained is that, for any  $\theta$  and  $F$ , the most unstable mode among all three-dimensional perturbations is always the two-dimensional sinuous Kelvin–Helmholtz (KH) mode ( $k_y = 0$ ). In other words, this mode is always more amplified than the two-dimensional varicose KH mode (odd  $w$ ), and three-dimensional instability modes. This result was *a priori* not obvious because when  $\theta$  is non-zero, there is no Squire’s theorem to guarantee that the most unstable modes are two-dimensional.

The characteristics of the most unstable mode as functions of the two base flow parameters  $F$  and  $\theta$  are summarized in figure 3. Figure 3(a) provides the maximum growth rate  $\omega_i$  while figures 3(b) and 3(c) give the associated oscillation frequency  $\omega_r$  and wavenumber  $k_x$  of the most unstable mode. The line  $F = 3\sqrt{3}/2$  which corresponds to  $Ri = 1/4$  is also indicated by a dashed line in these plots. As observed in figure 3(b,c), this line does correspond to a discontinuity associated with a change of mode, as further documented below.

Note first that for  $\theta = 0$ , the flow is stable for  $F < 3\sqrt{3}/2$ , that is, for  $Ri > 1/4$ . This is in agreement with the sufficient condition of stability obtained by Miles (1961) and

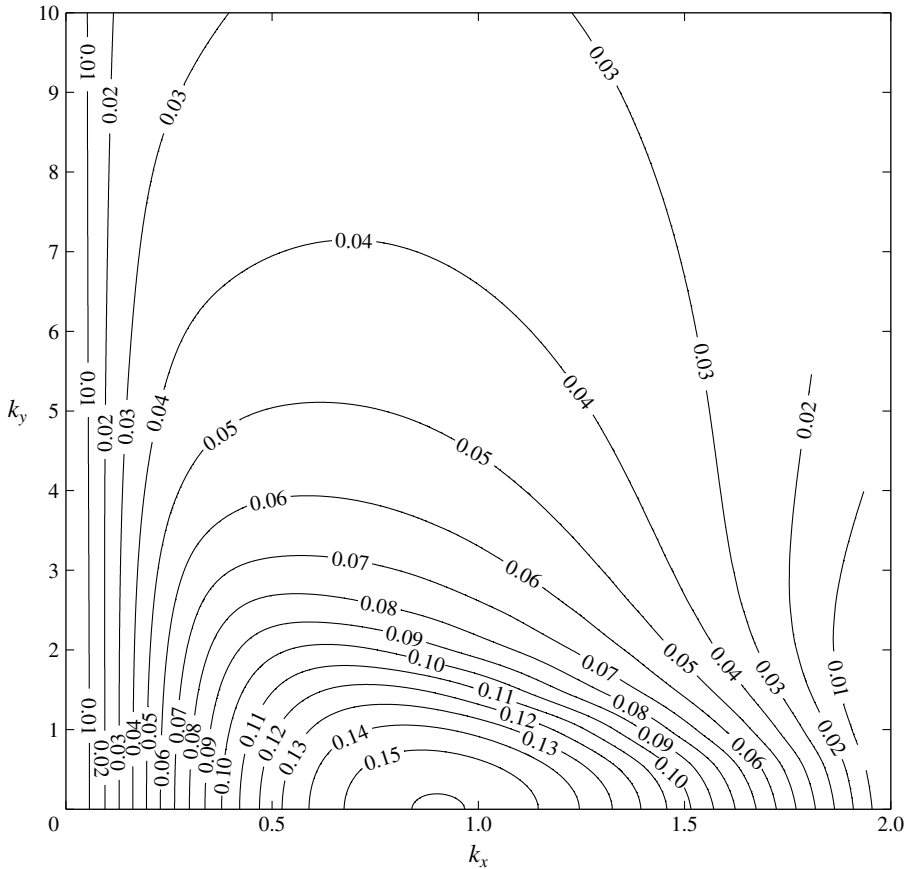


FIGURE 2. Growth rate of the sinuous KH mode in the  $(k_x, k_y)$  plane for  $\theta = \pi/2$  and  $F = 1$ .

Howard (1961). But when  $\theta \neq 0$ , the flow is unstable for any Froude number, that is, for any Richardson number. This means that, when the shear is not perfectly aligned in the direction of stratification, the condition of stability based on the Richardson number does not apply. This constitutes the second important result of the present paper.

The most unstable mode obtained for  $F > 3\sqrt{3}/2$  corresponds to the classical Kelvin–Helmholtz (KH) mode. Its characteristics are almost invariant with respect to  $\theta$  if we consider a fixed vertical Froude number  $F_v = F/\cos\theta$  in agreement with the asymptotic results obtained for large  $F$  in the previous section. This can be checked in figure 4(a), where the growth rate as a function of  $F_v$  is plotted for various  $\theta$ : we can see that for large  $F_v$ , the curves obtained for different  $\theta$  collide. Note that Jacobitz & Sarkar (1998) proposed a similar law in terms of Richardson number  $Ri_v = Ri \cos^2\theta$ , in the context of turbulent shear flows. But they probably did not consider sufficiently small Richardson numbers to be able to fit their data with this law.

Figure 4(a) shows that the most unstable mode is obtained for large vertical Froude numbers. It also demonstrates that for  $F < 3\sqrt{3}/2$  the unstable modes are strongly dependent of  $\theta$  but weakly sensitive to variations of  $F_v$ . This can also be seen on the growth rate plot shown in figure 4(b). On this plot, we observe that the growth rate curves collide for small  $F$  to a single curve given by (3.3) as expected from the small-Froude analysis.



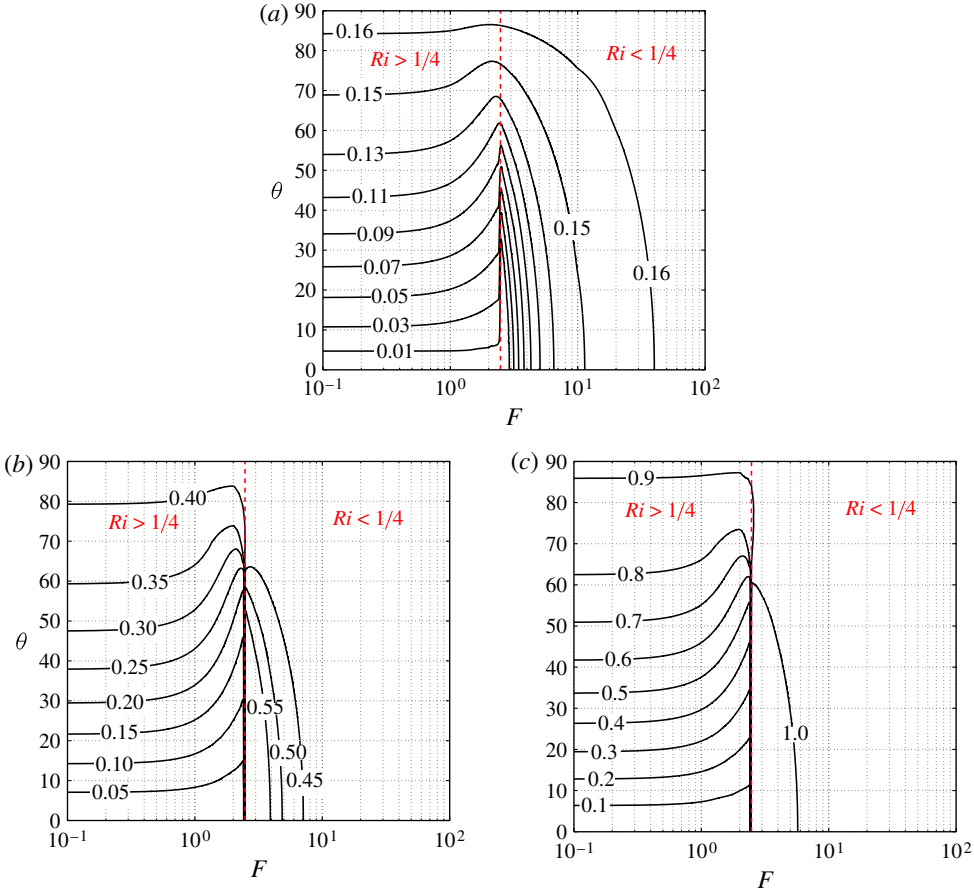


FIGURE 3. (Colour online available at [journals.cambridge.org/film](https://journals.cambridge.org/film)) Characteristics of the most unstable mode (two-dimensional sinuous KH mode) as functions of the base flow parameters  $\theta$  and  $F$ . (a) Growth rate  $\omega_i$ , (b) oscillation frequency  $\omega_r$ , (c) streamwise wavenumber  $k_x$ . The vertical dashed line given by  $F = 3\sqrt{3}/2$  corresponds to  $Ri = 1/4$  ( $Ri < 1/4$  for  $F$  on the right of this line).

Although the most unstable mode is always a two-dimensional sinuous KH mode, two different instability modes are involved. These two modes  $\omega^-$  and  $\omega^+$  are visible in figure 5, which shows the temporal branches versus  $k_x$  of the modes for  $F = 2.5$  and  $\theta = \pi/4$ . The two peaks associated with each mode on the growth rate curve are responsible for the jump in frequency and wavenumber observed in figure 3(b,c). Indeed, close to  $F = 3\sqrt{3}/2 \approx 2.6$ , these two peaks change their dominance and the most amplified wavenumber jumps from  $k_x \approx 0.5$  to  $k_x \approx 1.1$ . Note that the existence of two unstable modes associated with horizontal shear and vertical shear was also noticed by Blumen (1975) in his work on non-planar shear flows.

The spatial structure of the most unstable mode is displayed in figure 6 for various values of  $\theta$  and  $F$ . This figure shows the contour plots of the pressure field of the most unstable mode in the  $(x, z)$  plane. For small  $F$  (figure 6c,d), we can observe that the cross-stream structure (along  $z$ ) does not change with  $\theta$  or  $F$ , while the streamwise wavenumber increases with  $\theta$ . One could check that it varies according to  $\sin \theta$  as expected from the asymptotic analysis above. For large  $F$  (figure 6a,b), the



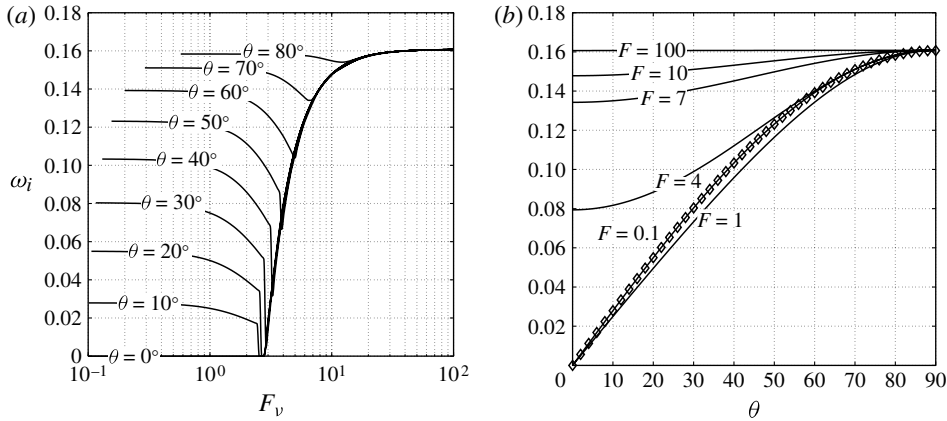


FIGURE 4. Characteristics of the most unstable mode (two-dimensional sinuous KH mode). (a) Growth rate as a function of  $F_v = F/\cos \theta$  for fixed inclination angles; (b) growth rate as a function of  $\theta$  for fixed Froude numbers. The symbols correspond to variations in  $\sin \theta$  as predicted by the small-Froude analysis.

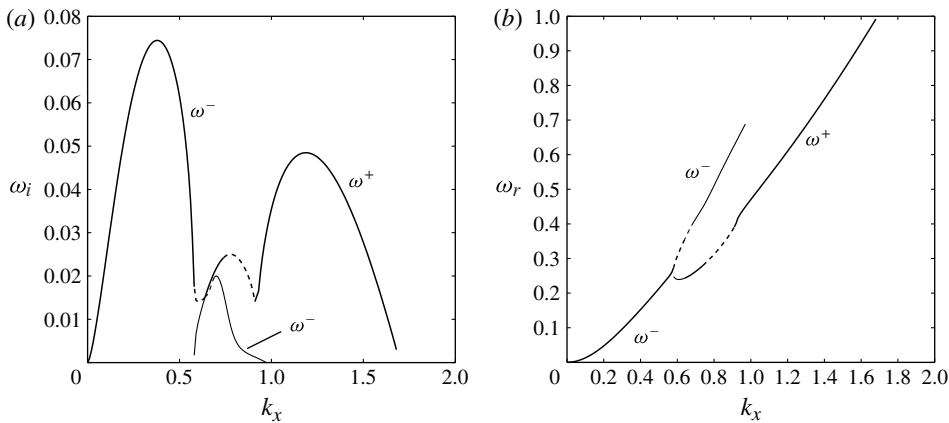


FIGURE 5. Growth rate  $\omega_i$  (a) and oscillation frequency  $\omega_r$  (b) versus  $k_x$  of the two-dimensional sinuous KH mode for  $F = 2.5$  and  $\theta = \pi/4$ . The two branches  $\omega^-$  and  $\omega^+$  associated with the most unstable modes are plotted. The modes are radiating (their oscillation frequency satisfies (2.8)) on the curve indicated by a dashed line. The dominant branch is plotted with a solid line. Here, the jump from one branch to the other occurs near  $k_x \approx 0.64$ .

cross-stream structure of the mode resembles the small  $F$  mode, but it is different owing to the presence of discontinuities. These discontinuities are associated with nearby critical points where  $\omega - k_x U = \pm \sin \theta / F$ . Note, however, that the other critical points associated with  $\omega - k_x U = 0$  or  $\omega - k_x U = \pm 1/F$  do not generate any apparent discontinuity on the pressure field of the mode. Nevertheless, those two other critical points are the local maxima of the eigenfunctions for  $F > 3\sqrt{3}/2$ , whereas the inflection point of the base flow is the only maximum for lower Froude numbers.

It is worth noting that none of the modes exhibits a radiative structure. This property was systematically checked: the oscillation frequency of the most unstable mode was never found to satisfy the condition (2.8). The most unstable mode is therefore never

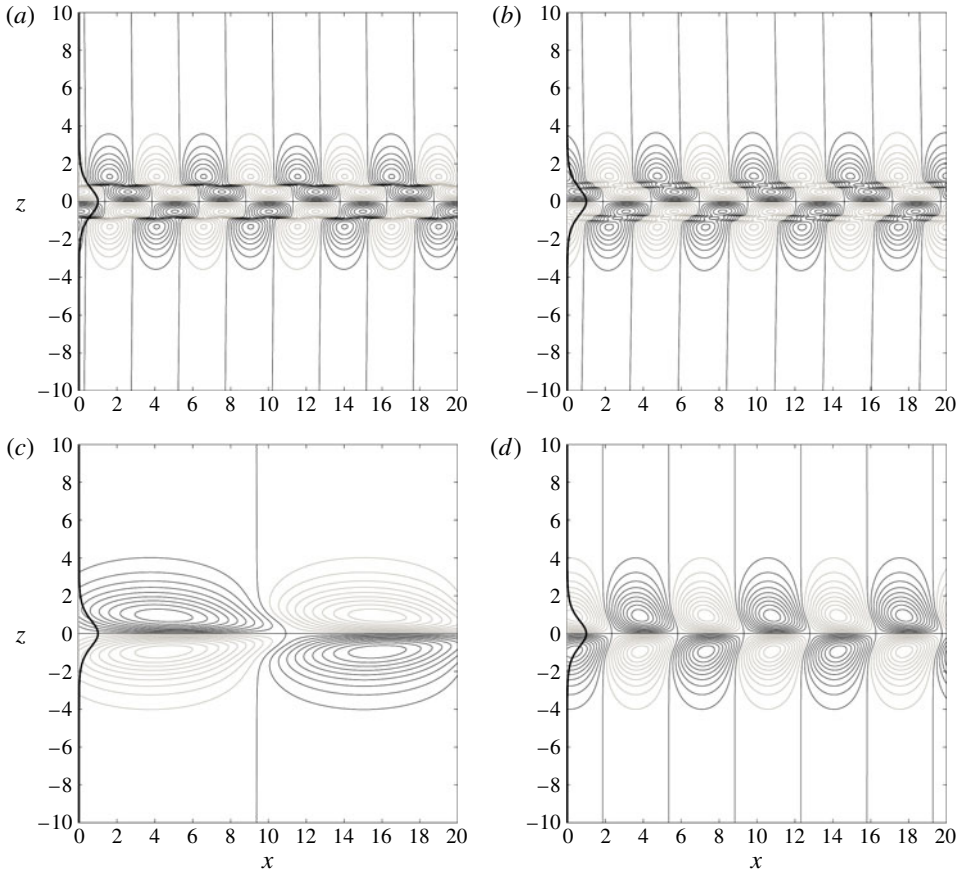


FIGURE 6. Spatial structure (pressure field) of the most unstable mode (two-dimensional sinuous KH mode). Pressure field contours of the normalized perturbation (contour values  $-1:0.1:1$ ). The jet velocity profile is also plotted on the left of each figure. (a)  $\theta = 0$ ,  $F = 3$ ,  $k_x = 1.2$ ,  $\omega = 0.599 + i0.0173$ ; (b)  $\theta = \pi/10$ ,  $F = 3$ ,  $k_x = 1.07$ ,  $\omega = 0.513 + i0.0214$ ; (c)  $\theta = \pi/10$ ,  $F = 0.1$ ,  $k_x = 0.287$ ,  $\omega = 0.132 + i0.0496$ ; (d)  $\theta = \pi/2$ ,  $F = 1$ ,  $k_x = 0.9023$ ,  $\omega = 0.407 + i0.16$ .

a radiative mode. In a complementary study (Candelier 2010), we show that unstable radiative modes do exist and we provide their characteristics.

## 5. Conclusion

The linear inviscid stability properties of a inclined stratified plane Bickley jet have been obtained for a large range of Froude numbers  $F$  and inclination angle  $\theta$ . First, we showed that when the direction of the shear is not aligned with the stratification, the jet is unstable for all Froude numbers. In particular, the Miles–Howard criterion for stability  $Ri > 1/4$  (that is,  $F < 3\sqrt{3}/2$ ) is not valid if  $\theta \neq 0$ . We found that the most unstable mode is always a two-dimensional non-radiating sinuous KH mode ( $k_y = 0$ ). The maximum growth rate was seen to be reached for large  $F$  (for any  $\theta$ ) or for  $\theta = \pi/2$  (for any  $F$ ). We have observed that the mode characteristics vary continuously with  $\theta$  but exhibit a jump associated with the presence of two peaks in the growth rate versus  $k_x$  curve when  $F$  passes the critical value  $F = 3\sqrt{3}/2$ , or equivalently when the Richardson number passes through  $1/4$ . Interestingly, this jump

occurs at approximately the same Richardson number for all  $\theta$ . On either side of this critical Richardson number, we have seen that the most unstable mode has simple characteristics. When  $Ri < 1/4$ , the characteristics of the most unstable mode are close to those obtained for small  $Ri$  (or large  $F$ ): they are the same as those of a vertical jet with the same length and velocity scales but with a modified Richardson number  $Ri_v = Ri \cos^2 \theta$ . When  $Ri > 1/4$ , the characteristics of the most unstable mode are close to those obtained for large  $Ri$  (or small  $F$ ) assuming  $\theta$  not too small. They are those of a horizontal jet with the same velocity scale but with a rescaled length scale,  $L_h = L/\sin \theta$ . In that case, there is no dependence on the Richardson number (or  $F$ ), but the growth rate, oscillation frequency and wavenumber are all proportional to  $\sin \theta$ .

Our analysis has focused on a particular jet profile, but we can reasonably argue that the results could be valid for other shear flows. Indeed, neither the asymptotic regimes describing the small and large  $Ri$  limits, nor the value of the critical Richardson number ( $Ri = 1/4$ ), depend on the base flow profile. Our results could then *a priori* apply to other jet profiles, and also to wakes and shear layers.

## REFERENCES

- ACHESON, D. J. 1976 On over-reflection. *J. Fluid Mech.* **77**, 433–472.
- BASAK, S. & SARKAR, S. 2006 Dynamics of a stratified shear layer with horizontal shear. *J. Fluid Mech.* **568**, 19–54.
- BASOVICH, A. Y. & TSIMRING, L. S. 1984 Internal waves in a horizontally inhomogeneous flow. *J. Fluid Mech.* **142**, 223–249.
- BLUMEN, W. 1971 Hydrostatic neutral waves in a parallel shear flow of a stratified fluid. *J. Atmos. Sci.* **28**, 340–344.
- BLUMEN, W. 1975 Stability of non-planar shear flow of a stratified fluid. *J. Fluid Mech.* **68**, 177–189.
- BOOKER, J. R. & BRETHERTON, F. P. 1967 The critical layer for internal gravity waves in a shear flow. *J. Fluid Mech.* **27**, 513–539.
- CANDELIER, J. 2010 Instabilités radiatives des jets et couches limites atmosphériques. PhD Thesis (in French).
- DELONCLE, A., CHOMAZ, J. M. & BILLANT, P. 2007 Three-dimensional stability of a horizontally sheared flow in a stably stratified fluid. *J. Fluid Mech.* **570**, 297–305.
- DRAZIN, P. G. & REID, W. H. 1981 *Hydrodynamic Stability*. Cambridge University Press.
- HOWARD, L. N. 1961 Note on a paper of John W. Miles. *J. Fluid Mech.* **10**, 509–512.
- JACOBITZ, F. G. & SARKAR, S. 1998 The effect of nonvertical shear on turbulence in a stably stratified medium. *Phys. Fluids* **10**, 1158–1168.
- JACOBITZ, F. G. & SARKAR, S. 1999 A direct numerical study of transport and anisotropy in a stably stratified turbulent flow with uniform horizontal shear. *Flow Turbul. Combust.* **63**, 343–360.
- LE DIZÈS, S. & BILLANT, P. 2009 Radiative instability in stratified vortices. *Phys. Fluids* **21**, 096602.
- LINDZEN, R. S. & BARKER, J. W. 1985 Instability and wave over-reflection in stably stratified shear flow. *J. Fluid Mech.* **151**, 189–217.
- LUO, K. H. & SANDHAM, N. D. 1997 Instability of vortical and acoustic modes in supersonic round jets. *Phys. Fluids* **9**, 1003–1013.
- MACK, L. M. 1990 On the inviscid acoustic-mode instability of supersonic shear flows. Part 1. Two-dimensional waves. *Theor. Comput. Fluid Dyn.* **2**, 97–123.
- MILES, J. W. 1961 On the stability of heterogeneous shear flows. *J. Fluid Mech.* **10**, 496–508.
- PARRAS, L. & LE DIZÈS, S. 2010 Temporal instability modes of supersonic round jets. *J. Fluid Mech.* **660**, 173–196.
- RIEDINGER, X., LE DIZÈS, S. & MEUNIER, P. 2010 Viscous stability properties of a Lamb–Oseen vortex in a stratified fluid. *J. Fluid Mech.* **645**, 255–278.